



**HAL**  
open science

# High Temperature Mechanical Properties of Ti(C, N)-Mo<sub>2</sub>C-Ni Cermets Studied by Internal Friction Measurements

T. Viatte, Thierry Cutard, G. Feusier, W. Benoit

► **To cite this version:**

T. Viatte, Thierry Cutard, G. Feusier, W. Benoit. High Temperature Mechanical Properties of Ti(C, N)-Mo<sub>2</sub>C-Ni Cermets Studied by Internal Friction Measurements. *Journal de Physique IV Proceedings*, 1996, 06 (C8), pp.C8-743-C8-746. 10.1051/jp4:19968161 . jpa-00254596

**HAL Id: jpa-00254596**

**<https://hal.science/jpa-00254596>**

Submitted on 4 Feb 2008

**HAL** is a multi-disciplinary open access archive for the deposit and dissemination of scientific research documents, whether they are published or not. The documents may come from teaching and research institutions in France or abroad, or from public or private research centers.

L'archive ouverte pluridisciplinaire **HAL**, est destinée au dépôt et à la diffusion de documents scientifiques de niveau recherche, publiés ou non, émanant des établissements d'enseignement et de recherche français ou étrangers, des laboratoires publics ou privés.

## High Temperature Mechanical Properties of Ti(C, N)-Mo<sub>2</sub>C-Ni Cermets Studied by Internal Friction Measurements

T. Viatte, T. Cutard\*, G. Feusier\* and W. Benoit\*

*Stellram S.A., Rte de l'Etraz, 1260 Nyon, Switzerland*

*\* Ecole Polytechnique Fédérale de Lausanne, Institut de Génie Atomique, 1015 Ecublens, Switzerland*

**Abstract:** internal friction measurements were performed on TiC<sub>0.7</sub>N<sub>0.3</sub>-Mo<sub>2</sub>C-Ni metal-bonded refractory materials, in order to study how the composition and the microstructure of cermets control the mechanical properties of these materials. A free inverted torsion-pendulum was used, oscillating in the 0.2-2 Hz frequency range, up to 1273K. Isothermal I.F. spectra were measured in a forced torsion-pendulum in the 10<sup>-10</sup> Hz range, and up to 1400K. One thermally activated I.F. peak at 1100K (at 0.5Hz), is superimposed with a high temperature I.F. background. The amplitude of the background and the activation energy of the peak are strongly dependent on the Mo and C content in the material. Transmission electronic microscope observations give complementary results to identify the relaxation mechanisms. In the physical model proposed to describe the anelastic behaviour of these materials, the 1100K peak is attributed to the dragging of Mo atoms by dislocations in Ni-Mo-Ti alloy, while the high temperature background is associated with long distance displacements of dislocations in this binder phase. The refractory skeleton gives a contribution to the high temperature background, and to another peak at 900K. A comparison is made with I.F. measurements in WC-Co, that confirms the specific role of the metallic phase for each system.

### 1. INTRODUCTION

The Ti(C,N)-Mo<sub>2</sub>C-Ni materials are appreciated for their good mechanical and chemical resistance in high speed machining. For these applications, the cutting tools have to stand mechanical stresses at high temperature (up to 1273K or more). Previous works [1] mentioned that the presence of molybdenum in the material enhances the resistance of these cermets to high temperature deformation. H. Matsubara [2] concluded that this would be mainly caused by the high Mo concentration in the metallic binder; no precise mechanism was proposed to explain it. M. Fährmann [3] established a correlation between the values of creep activation energy in TiC<sub>0.7</sub>N<sub>0.3</sub>-Mo<sub>2</sub>C-Ni cermets and the diffusion energy in nickel-molybdenum alloys. T. Viatte [4] presented a new experimental approach to understand the mechanisms involved in the deformation of each skeleton composing those materials. This approach uses internal friction and creep measurements to measure the high temperature mechanical properties. Both methods are used to compare the sintered materials to their isolated hard phase skeleton. The creep measurements and microscopic observations have already been presented [5]. This paper presents the results of internal friction measurements, giving complementary results to appreciate the role of the metallic binder phase in the resistance to deformation of cermets.

### 2. DESCRIPTION OF THE MATERIALS

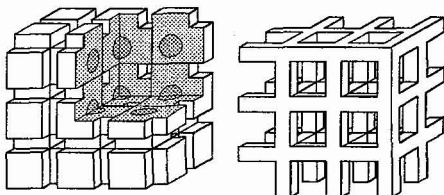


**Figure 1:** Schematic representation of the imbricated skeletons model, in the case of Ti(C,N)-Mo<sub>2</sub>C-Ni cermets.

On the left, the  $\gamma$  skeleton: carbide rims (Ti,Mo)(C,N) (light grey) embedding the carbonitride cores Ti(C,N) (dark grey);  
On the right, the  $\beta$  skeleton: Ni-Mo-Ti metallic alloy.

For some samples of each composition, a chemical extraction of the metallic binder was performed using a long time immersion, about 300 h, in a HCl+KClO<sub>3</sub> mixture maintained at 80°C.

The structure of the material is similar to the one of WC-Co. It can be schematically described as a metallic Ni-Mo-Ti skeleton, imbricated in the carbonitride hard phase skeleton, as illustrated in Figure 1. For this work, five different grades of TiC<sub>0.7</sub>N<sub>0.3</sub>-Mo-10%Ni cermets were fabricated at Stellram S.A. - Nyon, Switzerland, following a conventional powder metallurgy process. The physical characteristics of the sintered materials measured at room temperature are presented in Tab. 1.

Grade <sup>(1)</sup>					Metallic binder			Hard skeleton
	Mo content [wt.%]	grain size [ $\mu\text{m}$ ] <sup>(2)</sup>	HV 30 [ $\text{kg}/\text{mm}^2$ ]	crack length [ $\mu\text{m}$ ] <sup>(3)</sup>	d[111] binder [ $\text{\AA}$ ] <sup>(4)</sup>	Ti in binder [at.%] <sup>(5)</sup>	Mo in binder [at.%] <sup>(6)</sup>	Mo in (Ti,Mo)(C,N) rims [at.%] <sup>(7)</sup>
KONO	4.7	1.27	1575	146 $\pm$ 5	3.558	9.9 $\pm$ 0.6	2.3 $\pm$ 0.3	4.9 $\pm$ 0.6
KENO	9.4		1650	170 $\pm$ 5	3.579			
KINO	18.7	0.82	1725	192 $\pm$ 5	3.616	9.7 $\pm$ 0.8	16.9 $\pm$ 0.7	25.6 $\pm$ 0.2

Tab. 1. Chemical and mechanical characteristics of studied grades measured at room temperature. <sup>(\*)</sup> From statistical Ti(C,N) grain size distribution analysis on SEM micrographs of sintered structures. <sup>(\*\*)</sup> Mean length of Palmqvist cracks measured from the corners of HV30 indentations. <sup>(\*\*\*)</sup> From X-ray diffraction measurements on sintered materials. <sup>(\*\*\*\*)</sup> EDS analyses in Transmission Electronic Microscope.

The compositions, all with a common nickel content of 10 wt.% (corresponding to 6.4 vol.%), were chosen to study the influence of the Mo content, and the C content on the mechanical properties. All the studied materials were simultaneously sintered for 120 min. at 1723K. The sintering included a 60 min. sinterHIP step (30 bar argon pressure), to complete densification. The final dimensions of the samples (110 mm  $\times$  2.5 mm  $\times$  0.5 mm blades) were obtained by spark machining.

### 3. MEASUREMENT OF INTERNAL FRICTION

In a free oscillating mode, the internal friction (I.F.) is deduced from the logarithmic decrement of the amplitude decay. The dynamic shear modulus is deduced from the square of the frequency of oscillation. The torsional strain rate is  $\epsilon_{\theta} = 1.5 \cdot 10^{-5}$ , the vacuum is maintained better  $5 \cdot 10^{-5}$  Torr. Some measurements (see Figure 5) were realised in a subresonant forced oscillating mode, down to  $10^{-4}$  Hz. In this case, the internal friction is deduced from the direct measurement of the loss angle  $\delta$  between the applied stress  $\sigma$  and deformation  $\epsilon$ .

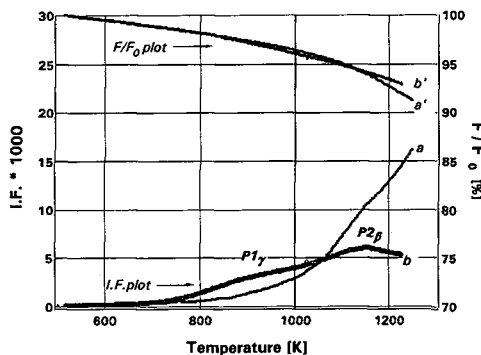


Figure 2: Internal friction and relative frequency measurements of  $\text{TiC}_{0.7}\text{N}_{0.3}\text{-Mo}_2\text{C-10 wt.\% Ni}$ . (a)KONO: 5wt.%  $\text{Mo}_2\text{C}$ , (b)KINO: 20wt.%  $\text{Mo}_2\text{C}$ . Free pendulum oscillating at  $F_0=2$  Hz. Heating at 2K/min.

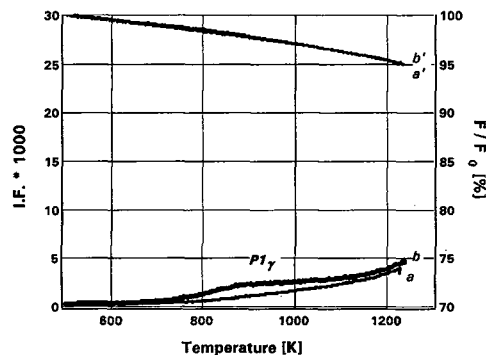


Figure 3: I.F. spectrum of  $\text{TiC}_{0.7}\text{N}_{0.3}\text{-(Ti,Mo)(C,N)}$  isolated skeletons, when the metallic binder is chemically removed. (a) KONO, (b) KINO.  $F_0=2$  Hz.

Typical I.F. and frequency measurements performed when heating  $\text{TiC}_{0.7}\text{N}_{0.3}\text{-Mo}_2\text{C-Ni}$  cermets are presented in Figure 2. When increasing the temperature, two peaks  $P1_\gamma$  at 950K and  $P2_\beta$  at 1150K are observed, superimposed with an exponential increase of the internal friction <sup>(2)</sup>. The amplitudes of the two peaks are higher for higher molybdenum contents (Figure 2). By contrast, the amplitude of the exponential I.F. background is higher for lower molybdenum content. This increase of internal friction at high temperature is associated with a severe decrease of the oscillation frequency, corresponding to a loss of the

<sup>(1)</sup> The designation of the grades have been chosen to classify the materials involved in the whole Stellram's research program: The second letter indicates the content of molybdenum carbide in the material: I for h<sub>igh</sub> level (here 18 vol.%), E for m<sub>edium</sub> (here 6.4 vol.%) and O for l<sub>ow</sub> level (here 3.2 vol.%).

<sup>(2)</sup> The subscript «  $\beta$  » is used because the peak is only observed in presence of the metallic binder ( $\beta$ -phase). The subscript «  $\gamma$  » is used when the peak is still observable in the isolated carbonitride skeleton ( $\gamma$ -phase), after chemical removal of the metallic binder. This notation is also used by G. Feusier in his work about  $\text{TiCN-Mo}_2\text{C-Co}$  cermets [6].

sample modulus. Figure 3 shows that in samples where the metallic skeleton is removed, the  $P2_{\beta}$  peak is absent, but  $P1_{\gamma}$  and a part of the exponential I.F. background remain. Comparing Figure 2 and Figure 3, it can be seen that at 1200K the contribution of the metallic binder to I.F. is predominant when the Mo content is low (curves a), but negligible when the Mo content is increased (curves b). Assuming the independence of the relaxation mechanisms between the two skeletons, one can deduce the specific contribution of the metallic binder by subtracting the curves of Figure 3 to those of Figure 2. One example of such a calculated spectrum is given in Figure 4. It is composed of one peak  $P2_{\beta}$  superimposed to one exponential background at high temperature. These calculated spectra for the metallic skeleton are very similar to I.F. measurements performed in different Ni-Mo alloys by V.N.Gridnev [7]. This similarity confirms that in the case of this material the I.F. contributions of the two skeletons are additive.

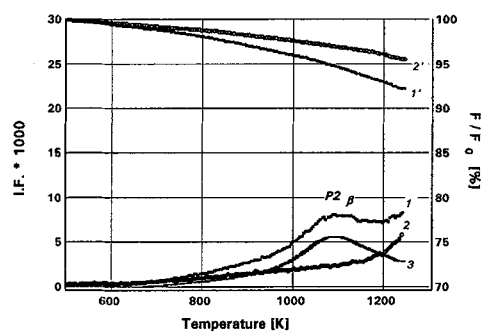


**Figure 4:** I.F. spectrum of KENO (1) before and (2) after removal of the metallic binder. Curve (3) is not experimental, but deduced by subtraction (3)=(1)-(2) pendulum oscillating at  $F_0=0.4$  Hz. Heating, 2K/min..

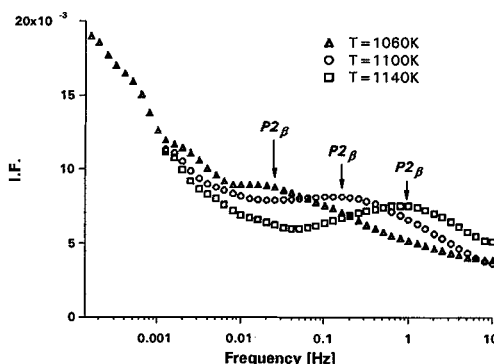


**Figure 5:** Isothermal I.F. spectra of complete KENO, in the activation conditions for the  $P2_{\beta}$  peak.

The isothermal I.F. spectra presented in Figure 5 are measured in a forced pendulum; each spectrum is obtained by varying the excitation frequency at a constant temperature. The temperature of  $P2_{\beta}$  is about 40K higher than in the free pendulum measurements, this is due to a different temperature calibration in the forced pendulum.  $P2_{\beta}$  corresponds to a thermally activated mechanism. The Arrhenius plot of the  $P2_{\beta}$  temperature provides an activation energy for the peak.:

$$E = -k \left. \frac{d(\ln \omega)}{d(1/T)} \right|_{T=T_p} \quad \text{where } \omega = 2\pi F \text{ is the pulsation of the pendulum, } k \text{ is the Boltzmann's constant.}$$

The energy obtained for  $P2_{\beta}$  is 3.6 eV for the low Mo cermets, and down to 2.9eV for the high Mo one. Respective relaxation times are  $8.10^{-18}$  and  $7.10^{-15}$  s. By contrast the  $P1_{\gamma}$  peak is not thermally activated. In its domain of temperature, no particular frequency dependence could be observed on I.F. level.

#### 4. DISCUSSION: THE DEFORMATION OF THE METALLIC BINDER

The anelastic behaviour of the metallic phase strongly depends on the quantity of molybdenum in the material. At high temperature, the reduction of the I.F. background (Figure 2) indicates that Mo has a strong hardening effect in the metallic binder phase. Furthermore, the Mo content changes the amplitude and the relaxation energy of the peak  $P2_{\beta}$ . This relaxation energy is close to the diffusion energy of metal atoms in Ni-Mo-Ti alloys, and it presents the same dependence toward the Mo content: increasing the Mo content also lowers the diffusion energy [8]. Nevertheless, the relaxation mechanism for  $P2_{\beta}$  cannot be a single point defect relaxation, since the amplitude  $\Delta$  of the  $P2_{\beta}$  peak does not present a regular dependence on the concentration of Mo atoms. For a point defect relaxation, one would indeed expect the dependence:  $\Delta \propto C_{PD}$  or  $(C_{PD})^2$ , where  $C_{PD}$  is the point defects concentration [9]. This is not the case for the  $P2_{\beta}$  peak: its amplitude is the highest for the intermediate composition KENO, and vanishes for higher and lower contents of molybdenum.

Assuming that  $P2_{\beta}$  is due to a dragging of Mo atoms by dislocations in nickel, one can understand that the amplitude of relaxation is related to both Mo content and dislocation density. Transmission electron microscopy observations performed in the binder of the cermets revealed that the dislocations are much more numerous in the case of low molybdenum cermets than in high Mo cermets. This explains that the amplitude of the  $P2_{\beta}$  peak is low in KINO (because the dislocation density is low), and in KONO (because the point-defect density is low). The amplitude is the highest when both dislocations and point defects are numerous in the binder phase, this is the intermediate case of KENO.

For such a dragging of Mo atoms, the relaxation energy naturally corresponds to the diffusion energy of Mo atoms in nickel-molybdenum alloys.

Nevertheless, a dragging of Mo atoms cannot be responsible for the hardening effect which is maintained at temperatures much higher than the peak. A hardening mechanism is proposed in Figure 6, resulting of the formation of jogs on the dislocations, in the special case of Ni-Mo alloys. In a pure nickel (Fig.6.1), the screw dislocations have different slip systems in the fcc structure, they can easily cross-slip, promoting the ductility of the material. Indeed, the stacking fault energy ( $\gamma_{SF}$ ) is high, and the dislocations are not dissociated. In Ni-Mo alloys (Fig.6.2)  $\gamma_{SF}$  is much lower than in pure Ni [10, 11]. The dislocations can therefore be locally dissociated when encountering molybdenum atoms. Since the distribution of the Mo atoms is random in the crystal, different segments of one dislocation can be dissociated in different planes. The pinning of the dislocations by the jogs between those segments (Fig.6.3) constitutes a hardening of the binder phase. In Fig.6.4, when the diffusion of the Mo atoms becomes possible, the dissociated dislocation segments can oscillate between the jogs and drag the Mo atoms. This gives rise to the  $P2_{\beta}$  peak. The motion of the whole dislocation implies the migration of the jogs. Needing a long distance migration of vacancies, this motion is only possible at higher temperature. It gives rise to the plastic deformation of the metallic binder, and to the exponential increase of the internal friction at high temperature.

This model presents some similarities with the model developed by Ammann and Schaller for the cobalt binder in WC-Co. The dissociation of the dislocations results in this case of the allotropic hc-fcc transformation of cobalt [12, 13, 14].

## 5. CONCLUSION

The presence of molybdenum in nickel strongly hardens the alloy up to high temperature. Furthermore the molybdenum promotes a relaxation mechanism that is expected to enhance the toughness of the alloy when used as a binder phase for Ti(C,N)-Mo<sub>2</sub>C-Ni cermets. The relaxation mechanisms in Ni-Mo-Ti metallic binders are similar to those observed in the cobalt binder of WC-Co, but they are shifted to higher temperature.

## Acknowledgements

The authors are grateful to Dr. K. Stjernberg (Stellram S.A.) for his useful discussions. This work was financially supported by Stellram S.A., Nyon (Switzerland), and by the Swiss « Commission pour l'Encouragement de la Recherche Scientifique »

## References

- [1] H. Suzuki, M. Saito, O. Terada, *et al.*, *J. Jap. Soc. of P&PM*, **40**(7)(1993). p. 739-742.
- [2] H. Matsubara, *J. Hard Mater.*, **3**(3-4)(1991). p. 339-350.
- [3] M. Fährmann, *Int. J. Refr. Metals & Hard Mat.*, (12)(1989). p. 219-223.
- [4] T. Viatte, (1995), THESE EPFL N°1371, Département de Physique, Lausanne, Switzerland.
- [5] T. Cutard, T. Viatte, G. Feusier, *et al.*, *Material Science and Engineering A*, (1996).
- [6] G. Feusier, T. Cutard, C. Verdon, *et al.* in ICIFUAS'96. (1996). Poitiers: July 7-11, 1996, *In this issue*.
- [7] V.N. Gridnev and N.P. Kushnareva. in Proceeding of ICIFUAS-9. (1989). p. 141-144.
- [8] Smitthells, in *Metals Reference Handbook*. (1983). p. 13/47-13/49.
- [9] A.S. Nowick and B.S. Berry, *Anelastic Relaxation in Crystalline Solids*, Academic Press, New York, (1972).
- [10] K. Ishida, *Phil. Mag.*, **32**(3)(1975). p. 663-670.
- [11] T.C. Tearnay and N.J. Grant, *Metall. Trans. A*, **13A**(October)(1982). p. 1827-1836.
- [12] J.J. Ammann and R. Schaller, *J. Alloys Compounds*, (211/212)(1994). p. 397-401.
- [13] J.J. Ammann, D. Mari, R. Schaller, *et al.* in Proc. of 9th Risø Int. Symp. Met. & Mat. Science. (1988). p. 257-262.
- [14] J.J. Ammann, (1990), THESE EPFL N°861, Département de physique, Lausanne, Switzerland.

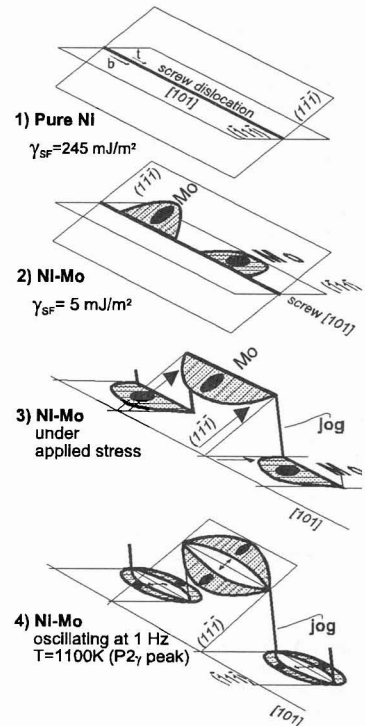


**Figure 6:** Scheme of the interaction between one dislocation and Mo atoms (dark spots) in nickel. The grey zones are planar faults resulting of the dissociation of the dislocation.